Clay Minerals (2020), **55**, 96–100
doi:10.1180/clm.2020.8

CAMBRIDGE UNIVERSITY PRESS

Brief Report

Thermal degradation kinetics of sepiolite

Yüksel Sarıkaya[1], Müşerref Önal[1]* and Abdullah Devrim Pekdemir[2]

[1]Ankara University, Faculty of Science, Department of Chemistry, Tandoğan, 06100 Ankara, Turkey and [2]Ankara University, Graduate School of Natural and Applied Sciences, Dışkapı, 06110, Ankara, Turkey

Abstract

The kinetic parameters of the thermal degradation of sepiolite were evaluated with a new method based on thermal analysis data. Thermogravimetric/differential thermal analysis curves were recorded for the natural and preheated sepiolite samples in the temperature range 25–800°C for 4 h. The temperature-dependent height of the exothermic heat flow peak for the thermal decomposition of sepiolite located at ~850°C on the differential thermal analysis curve was taken as a kinetic variable for the thermal degradation. A thermal change coefficient was defined depending on this variable because this coefficient fit to the Arrhenius equation was assumed as a rate constant for the thermal degradation. The Arrhenius plot showed that the degradation occurs in three steps. Two of these are due to stepwise dehydration and the third originated from dehydroxylation of sepiolite. Three activation energies were obtained that increase with the increasing temperature interval of the steps.

Keywords: decomposition, degradation, kinetics, sepiolite, thermal analysis

(Received 17 May 2019; revised 9 March 2020; Accepted Manuscript online: 13 March 2020; Associate Editor: Asuman Turkmenoglu)

Sepiolite is a fibrous clay mineral with an ideal chemical formula per half unit cell of $Si_{12}O_{30}Mg_8(OH)_4(OH_2)_4.xH_2O$, where x is usually 8 and decreases depending on the drying temperature and applied vacuum (Brauner & Preisinger, 1959). The xH_2O, $(OH_2)_4$ and $(OH)_4$ groups are zeolitic water, hydroxyls along the edges of the octahedral strip and hydroxyls in the inner octahedral strips, respectively (Ahlrichs *et al.*, 1975; Prost, 1975; Kiyohiro & Otsuka, 1989; Frost & Ding, 2003). Zeolitic water occupies the inter-channels *via* consecutive multi-molecular adsorption and then capillary condensation. Physical bonds between the magnesium cations and hydroxyls along the edges of the octahedral strip originate from the ion-dipole attractive forces. By contrast, covalent bonds exist between the structural hydroxyls and magnesium atoms. Synthetic sepiolite may be synthesized from SiO_2 gel and magnesium chloride (Jeans, 1971; Aetahi, 1985).

In the past, several studies have been carried out on the dehydration, dehydroxylation and decomposition of sepiolite (Perraki & Orfanoudaki, 2008; Ogorodova *et al.*, 2014; Wang *et al.*, 2014). The changes in the various physicochemical properties of sepiolite after heating in air and under vacuum have been examined extensively (McCarter *et al.*, 1950; Kulbicki, 1959; Dandy & Nadiye-Tabbiruka, 1975; Shuali *et al.*, 1991). The effects of heating, acid leaching and various chemical treatments on the crystal structure and properties of sepiolite have been discussed qualitatively (Serna *et al.*, 1975; Yebra-Rodriquez *et al.*, 2003; Yılmaz *et al.*, 2013, Fitaroni *et al.*, 2019). Sepiolite has been used widely in many processes, such as adsorption, catalysis, bleaching of edible oils, clarification of fruit juices, preparation of polymer nanocomposites and pharmaceutical applications (Galan, 1996; Murray, 1999; Saneeri *et al.*, 2015, González-Santamaria, 2017; Mirzaaghaei *et al.*, 2017; Al-Ani *et al.*, 2018; Tian *et al.*, 2019).

Major sepiolite deposits occur in the USA, Spain, France and Turkey. The geology and genesis of sepiolite deposits mined in the Eskişehir (Turkey) zone have been investigated extensively (Ece & Çoban, 1994). The Eskişehir sepiolite, known as pipestone, has a white colour. The physicochemical properties of this material, such as the chemical and mineralogical composition, thermal shrinkage, particle morphology and size distribution of nano- and macro-pores, have been determined (Yener *et al.*, 2007; Önal *et al.*, 2008). In addition, the modification of some of these properties depending on the applied acid treatment has been investigated (Çetişli & Gedikbey, 1990; Inukai *et al.*, 1994; Erdoğan *et al.*, 1996), and the influence of heating on the crystal structure, porosity, sintering surface structure and catalytic properties of sepiolite have been discussed (Göktaş *et al.*, 1997; Balcı, 1999; Yılmaz *et al.*, 2013; Meşe *et al.*, 2018). Despite there being several experimental and theoretical interpretations, a numerical analysis of the thermal degradation of sepiolite crystals has not yet been performed extensively. Thus, the aim of this contribution is to use thermal analysis data to estimate some of the physicochemical parameters of the thermal degradation of sepiolite that accompany dehydration and dehydroxylation.

Material and methods

A sample of Eskişehir sepiolite was ground gently in a mortar and air dried at room temperature for 1 week. The air-dried samples, each having a mass of 10 g, were heated at pre-set temperatures within the range of 25–1000°C for periods of 4 h.

The chemical analysis of the sample after heating at 100°C for 2 h was carried out using a Hitachi Z-8200 Atomic Absorption

*Email: onal@science.ankara.edu.tr
Cite this article: Sarıkaya Y, Önal M, Pekdemir AD (2020). Thermal degradation kinetics of sepiolite. *Clay Minerals* **55**, 96–100. https://doi.org/10.1180/clm.2020.8

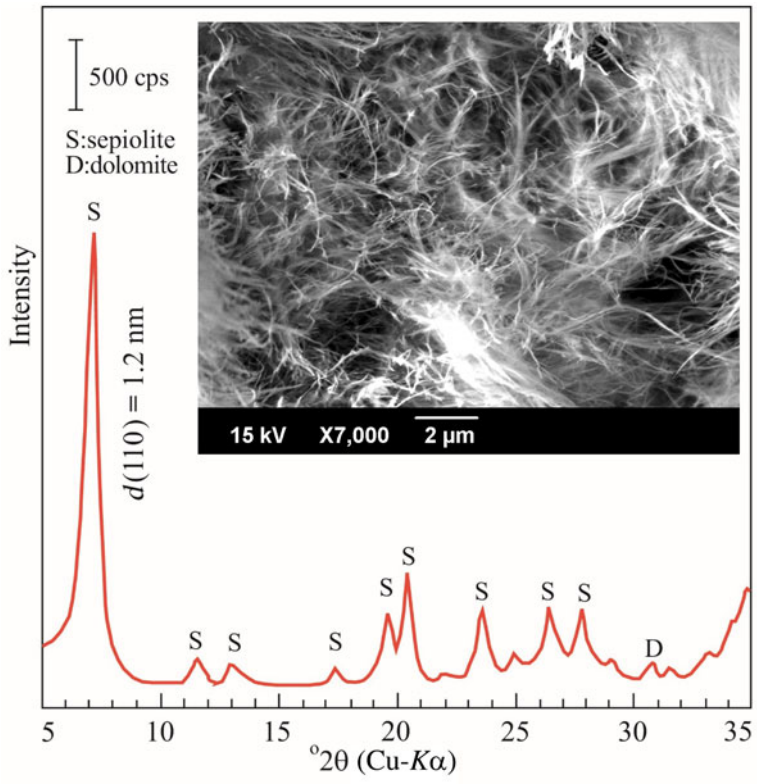

Fig. 1. XRD trace and SEM image of the sepiolite.

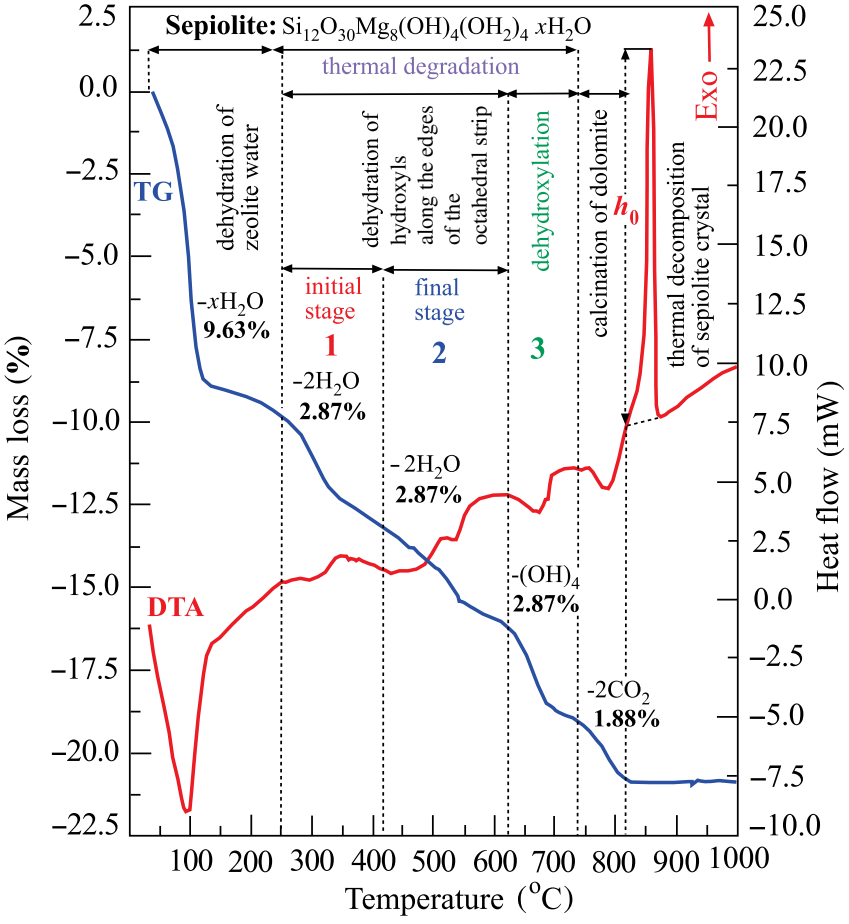

Fig. 2. Thermal degradation steps of the sepiolite as shown in the TG/DTA curves.

https://doi.org/10.1180/clm.2020.8 Published online by Cambridge University Press

Spectrophotometer. The X-ray diffraction (XRD) trace of the natural sepiolite was obtained from random mounts using a Rigaku D-Max 2200 Powder Diffractometer with Cu-*K*α radiation and a Ni filter. The morphology of the sample was examined by scanning electron microscopy (SEM) using a JEOL JSM-490LV instrument operating at an accelerating voltage of 15 kV. Thermogravimetric and differential thermal analysis (TG/DTA) curves were recorded for the natural and heated samples between 25°C and 1000°C under atmospheric pressure with a heating rate of 10°C min^{-1} using a Setaram Instrument (Labsys SETSYS-1780).

Results and discussion

Mineralogy, morphology and chemical composition of the sepiolite

A SEM image and XRD trace of the sepiolite are shown in Fig. 1. The SEM image shows the fibrous morphology and porous texture of the sepiolite. The XRD trace indicates that the sepiolite contains minor dolomite ($CaMg(CO_3)_2$) impurities. The chemical analysis of the sepiolite (mass%) was: SiO_2 (57.60), MgO (25.06), Al_2O_3 (1.85), Fe_2O_3 (0.55), TiO_2 (0.13), CaO (0.86), Na_2O (0.08), K_2O (0.15) and loss on ignition (13.20). The abundance of dolomite was estimated to be 3% from the CaO content. The Al_2O_3 and Fe_2O_3 are due to the partial replacement of Mg^{2+} by Al^{3+}, Fe^{2+} and Fe^{3+} in sepiolite.

Thermal analysis

The TG/DTA curve of the sepiolite is given in Fig. 2. The temperature intervals and mass-loss percentages for the dehydration, dehydroxylation, thermal degradation and thermal decomposition of the sepiolite and decomposition dolomite are also shown in Fig. 2. The removal of hydroxyls along the edges of the octahedral strip occurs in two steps and the removal of hydroxyls from the inner octahedral strips of the sepiolite are endothermic, whereas its thermal decomposition is strongly exothermic (Fig. 2).

The TG/DTA curves of the heated samples showed that the exothermic heat flow for the thermal decomposition decreases at preheating temperatures >250°C (Fig. 3). The heights (h) of the heat-flow peaks for various preheating temperatures are listed in Table 1. The plot of h against temperature showed that the structure of the sepiolite remained unchanged at <250°C and then degraded linearly (Fig. 4). The equation and slope for the straight line obtained were determined from Eqs (1) and (2), respectively:

$$h = -0.051T + 51.867 \quad (1)$$

$$(\partial h/\partial T)_p = -0.051 \text{ mW K}^{-1} \quad (2)$$

where the subscript p represents the atmospheric pressure, which is constant in the thermal treatments.

Kinetic considerations

A thermal degradation coefficient is proposed from Eq. (3):

$$k = -\frac{1}{h}\left(\frac{\partial h}{\partial T}\right)_p \quad (3)$$

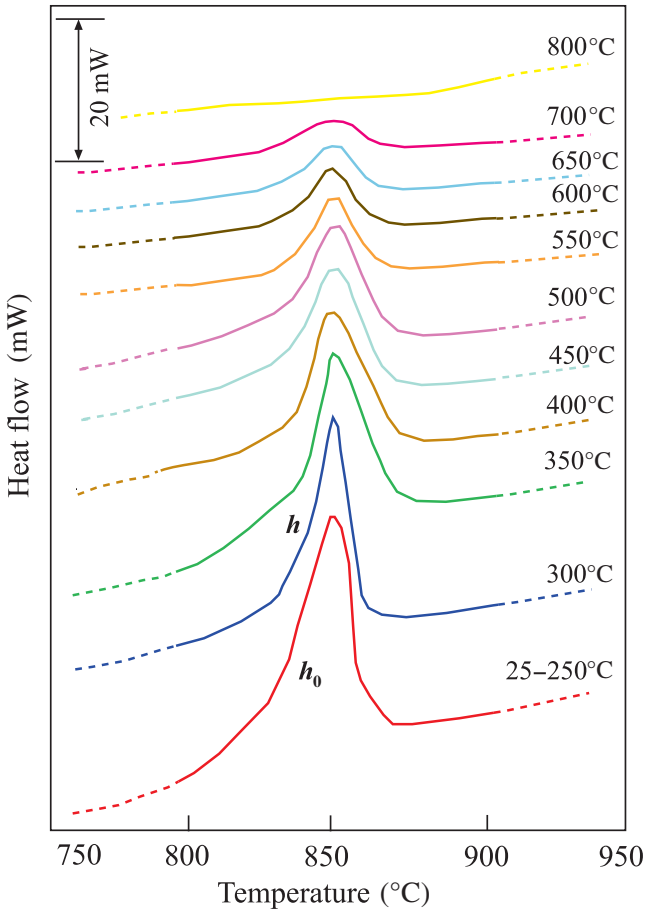

Fig. 3. Heat flow (h) *vs* increasing preheating temperature for the exothermic thermal decomposition of the sepiolite.

by analogy from the thermal expansion and isothermal compression coefficients. As $(\partial h/\partial T)_p < 0$, the negative sign is incorporated into the definition so that k is positive. This is not required in the case of this derivative being positive.

The k and ln$k$ values for each preheating temperature calculated from Eq. (3) are listed in Table 1. The projection of ln$k$ against $1/T$ shows three consecutive intersecting straight lines (Fig. 5). The presence of straight lines suggests that the k coefficient might be considered to be similar to the reaction rate constant. Thus, each straight line should fit to the Arrhenius

Table 1. Kinetic and thermodynamic parameters obtained from the thermal analysis of the sepiolite ($k = -(\partial h/\partial T)/h$, $h_0 = 24$ mW and $(\partial h/\partial T)_p = -0.051$ mW/K).

T (K)	$1/T$ (10^{-3} K^{-1})	h (mW)	k (10^{-3} K^{-1})	ln$k$
523	1.912	24.0	2.125	–6.154
573	1.745	23.0	2.217	–6.111
623	1.605	20.0	2.550	–5.972
673	1.486	17.5	2.914	–5.838
723	1.383	15.0	3.400	–5.684
773	1.294	12.0	4.250	–5.461
823	1.215	10.0	5.100	–5.279
873	1.146	7.0	7.286	–4.922
923	1.083	5.0	10.200	–4.585
973	1.028	2.5	20.400	–3.892

https://doi.org/10.1180/clm.2020.8 Published online by Cambridge University Press

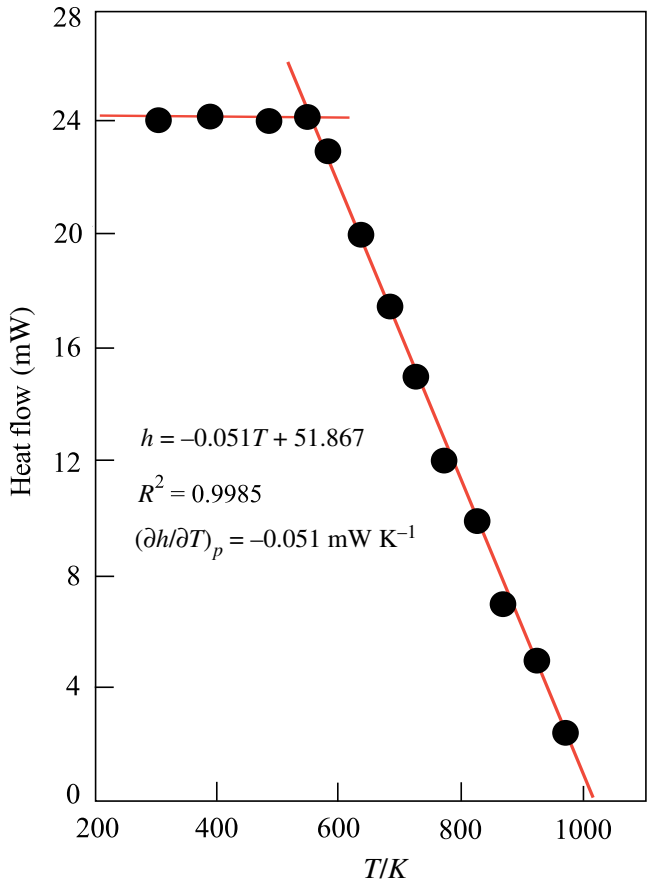

Fig. 4. Heat flow (h) *vs* absolute preheating temperature (T) for the thermal decomposition of the sepiolite.

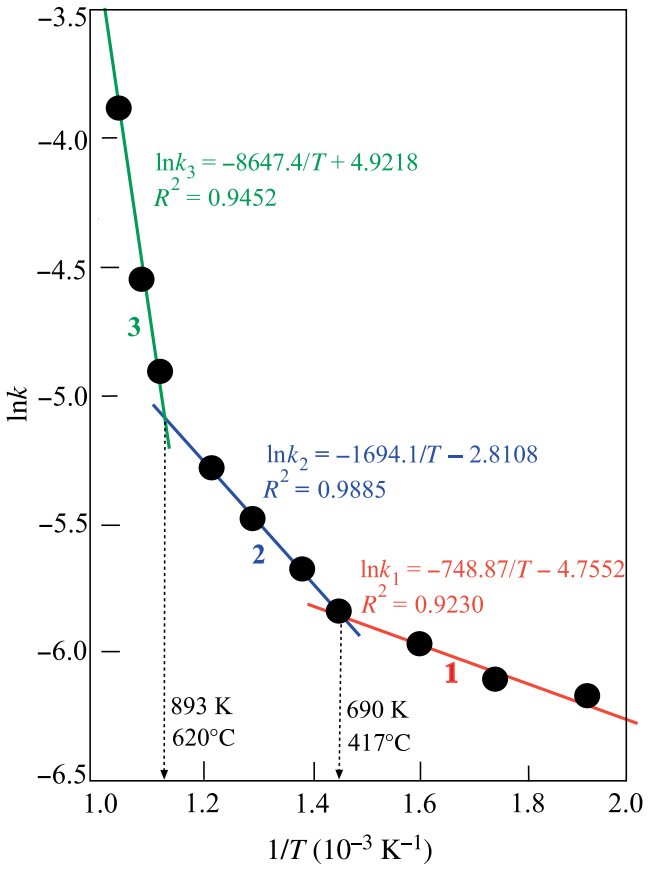

Fig. 5. Arrhenius graphs showing three intersecting straight lines obtained from ln$k$ *vs* 1/T.

equation in Eq. (4):

$$\ln k = \ln A - E^{\#}/RT \quad (4)$$

where A is the pre-exponential frequency factor, $E^{\#}$ is the activation energy (J mol^{-1}), T is the absolute temperature (K) and R = 8314 J mol^{-1} K^{-1} is the universal gas constant.

The intersect temperatures and the equations of the straight lines are shown in Fig. 5. The first term of each equation should be equal to the ln$A$ value. The corresponding $E^{\#}$ values were calculated from the slopes, being equal to $-E^{\#}/R$. Using the calculated ln$A$ and $E^{\#}$ values, three Arrhenius equations (Eqs 5–7) and corresponding temperature intervals were obtained:

$$\ln k_1 = -4.7552 - 6226/RT, \quad 250–417^{\circ}C \quad (5)$$

$$\ln k_2 = -2.8108 - 16\,941/RT, \quad 417–620^{\circ}C \quad (6)$$

$$\ln k_3 = 4.9218 - 71\,894/RT, \quad 620–730^{\circ}C \quad (7)$$

The three different activation energies and the corresponding Arrhenius equations indicated that the change proceeds *via* three consecutive mechanisms that result in the thermal degradation of sepiolite.

The first and second mechanisms result from the two consecutive stages of removal of hydroxyls along the edges of the octahedral strip. The various activation energies are attributed to the various positions and orientations of the H_2O molecules physically bonded to magnesium cations in the intra-fibre channels of the sepiolite crystal. The greater value of $E_3^{\#}$ compared to $E_1^{\#}$ and $E_2^{\#}$ is due to the chemical nature of the dehydroxylation, whereas dehydration is a physical process. Similar results were obtained using the intensity of the most characteristic XRD reflection of sepiolite (110) as a kinetic variable (Kiyohiro & Otsuka, 1989; Perraki & Orfanoudaki, 2008; Sarıkaya *et al.*, 2019; Tian *et al.*, 2019).

Conclusions

The temperature-dependent h of any exothermic or endothermic heat-flow peak on the DTA curve may be used to calculate the kinetic parameters of the thermal degradation of minerals. The volume, density, porosity, surface area, micro-hardness, intensity of any XRD peak and other mechanical properties that change linearly with temperature may also be used as system variables instead of the peak h of the heat flow. The possible apparent activation energies as well as the path of degradation with one or more step(s) could be evaluated from a thermal coefficient that is comparable to a reaction rate constant.

Financial support. This research was supported by Ankara University Scientific Research Projects Coordination Unit (Project No.: 12B4240016).

https://doi.org/10.1180/clm.2020.8 Published online by Cambridge University Press

References

Aetahi A. (1985) Synthesis of sepiolite at room temperature from SiO_2 and $MgCl_2$ solution. *Clay Minerals*, **20**, 521–523.

Ahlrichs J.L., Serna C. & Serratosa J.M. (1975) Structural hydroxyls in sepiolites. *Clays and Clay Minerals*, **23**, 119–124.

Al-Ani A., Gertisser, R. & Zholobenko, V. (2018) Structural features and stability of Spanish sepiolite as a potential catalyst. *Applied Clay Science*, **162**, 297–304.

Balcı S. (1999) Effect of heating and pre-treatment on pore size distribution of sepiolite. *Clay Minerals,* 34, 647–655.

Brauner K. & Preisinger A. (1959) Structur und entstehung des sepioliths. *Tschermaks Mineralogische und Petrographische Mitteilungen,* 6, 120–140.

Çetişli H. & Gedikbey T. (1990) Dissolution, kinetics of sepiolite from Eskişehir (Turkey) in hydrochloric and nitric acids. *Clay Minerals*, **25**, 207–215.

Dandy A.J. & Nadiye-Tabbiruka M.S. (1975) The effect of heating *in vacuo* on the microporosity of sepiolite. *Clays and Clay Minerals,* 23, 428–430.

Ece Ö.I. & Çoban F. (1994) Geology, occurrence, and genesis of Eskişehir sepiolites, Turkey. *Clays and Clay Minerals*, **42**, 81–92.

Erdoğan B., Demirci Ş. & Akay Y. (1996) Treatment of sugar beet juice with bentonite, sepiolite, diatomite, and quartamin to remove color and turbidity. *Applied Clay Science*, **11**, 55–67.

Fitaroni L.B., Venâncio T., Tanaka F.H., Gimenez J.C.F., Costa J.A.S. & Cruz S.A. (2019) Organically modified sepiolite: thermal treatment and chemical and morphological properties. *Applied Clay Science*, **179**, 1–10.

Frost R.L. & Ding Z. (2003) Controlled rate thermal analysis and differential scanning calorimetry of sepiolites and palygorskites. *Thermochimica Acta*, **397**, 119–128.

Galan E. (1996) Properties and applications of palygorskite-sepiolite clays. *Clay Minerals,* 31, 443–453.

Göktaş A.A., Mısırlı Z. & Baykara T. (1997) Sintering behaviour of sepiolite. *Ceramics International*, **23**, 305–311.

González-Santamaria, D.E., Lopez E., Ruiz A., Fernández R., Ortega A. & Cuevas, J. (2017) Adsorption of phenanthrene by stevensite and sepiolite. *Clay Minerals*, **52**, 341–350.

Inukai K., Miyawaki R., Tomura S., Shimosaka K. & Irkeç T. (1994) Purification of Turkish sepiolite through hydrochloric acid treatments. *Applied Clay Science*, **9**, 11–29.

Jeans C.V. (1971) The neoformation of clay minerals in brackish and marine environments. *Clay Minerals*, **9**, 209–217.

Kiyohiro T. & Otsuka R. (1989) Dehydration mechanism of bound water in sepiolite. *Thermochimica Acta*, **147**, 127–138.

Kulbicki G. (1959) High temperature phases in sepiolite, attapulgite and saponite. *American Mineralogist*, **44**, 752–758.

McCarter W.S.W., Krieger K.A. & Heinemann H. (1950) Thermal activation of Attapulgus clay: effect on physical and adsorptive properties. *Industrial and Engineering Chemistry*, **42**, 529–533.

Meşe E., Figen A.K., Filiz B.C. & Pişkin S. (2018) Cobalt–boron loaded thermal activated Turkish sepiolite composites (Co–B@tSe) as a catalyst for hydrogen delivery. *Applied Clay Science*, **153**, 95–106.

Mirzaaghaei M., Goli S.A.H. & Fathi G. (2017) Clarification of apple juice using activated sepiolite as a new fining clay. *Clay Minerals*, **52**, 497–508.

Murray H.H. (1999) Applied clay mineralogy today and tomorrow. *Clay Minerals*, **34**, 39–49.

Ogorodova L.P., Kiseleva I.A., Vigasina M.F., Kabalov Y.K., Grishchenko R.O. & Mel'chakova L.V. (2014) Natural sepiolite: enthalpies of dehydration, dehydroxylation, and formation derived from thermochemical studies. *American Mineralogist*, **99**, 2369–2373.

Önal M., Yılmaz H. & Sarıkaya Y. (2008) Some physicochemical properties of the white sepiolite known as pipestone from Eskişehir, Turkey. *Clays and Clay Minerals*, **56**, 511–519.

Perraki T. & Orfanoudaki A. (2008) Study of raw and thermally treated sepiolite from the Mantoudi area, Euboea, Greece: X-ray diffraction, TG/DTG/DTA and FTIR investigations. *Journal of Thermal Analysis and Calorimetry*, **91**, 589–593.

Prost R. (1975) Infrared study of the interactions between the different kinds of water molecules present in sepiolite. *Spectrochimica Acta,* 31A, 1497–1499.

Saneeri M., Goli S.A.H. & Keramat J. (2015) Optimization of oil bleaching parameters using response surface methodology, for acid-activated sepiolite from Iran. *Clay Minerals*, **50**, 639–648.

Sarıkaya Y., Önal M. & Pekdemir A.D. (2019) Kinetic and thermodynamic approaches on thermal degradation of sepiolite crystal using XRD-analysis. *Journal of Thermal Analysis and Calorimetry* (epub ahead of print) DOI: 10.1007/s10973-019-09053-3.

Serna C., Ahlrichs J.L. & Serratosa J.M. (1975) Folding in sepiolite crystals. *Clays and Clay Minerals*, **23**, 452–457.

Shuali U., Yariv S., Steinberg M. & Müller-Vanmoos M. (1991) Thermal analysis of pyridine-treated sepiolite and palygorskite. *Clay Minerals*, **26**, 497–506.

Tian G., Han G., Wang F. & Liang J. (2019) Sepiolite nanomaterials: structure, properties and functional applications. Pp. 135–201 in *Nanomaterials from Clay Minerals* (A. Wang & W. Wang, editors). Elsevier, Amsterdam, The Netherlands.

Wang F., Liang J., Tang Q., Chen C. & Chen, Y. (2014) Channel microstructure and thermal insulation mechanism of sepiolite mineral nanofibers. *Journal of Nanoscience and Nanotechnology*, **14**, 3937–3942.

Yebra-Rodriquez A. Martin-Ramos J.D., Del Rey F., Viseras C. & Lopez-Galindo A. (2003) Effect of acid treatment on the structure of sepiolite. *Clay Minerals*, **38**, 353–360.

Yener N., Önal M., Üstünışık G. & Sarıkaya Y. (2007) Thermal behavior of a mineral mixture of sepiolite and dolomite. *Journal of Thermal Analysis and Calorimetry*, **88**, 813–817.

Yılmaz M.S., Kalpaklı Y. & Pişkin S. (2013) Thermal behavior and dehydroxylation kinetics of naturally occurring sepiolite and bentonite. *Journal of Thermal Analysis and Calorimetry*, **114**, 1191–1199.

https://doi.org/10.1180/clm.2020.8 Published online by Cambridge University Press